J Mol Model (2013) 19:2885–2891
DOI 10.1007/s00894-012-1706-7

ORIGINAL PAPER

Influence of the monoclinic and tetragonal zirconia phases on the water gas shift reaction. A theoretical study

María Luisa Cerón · Barbara Herrera · Paulo Araya · Francisco Gracia · Alejandro Toro-Labbé

Received: 27 July 2012 / Accepted: 20 November 2012 / Published online: 2 February 2013

Abstract We present a theoretical study of the water gas shift reaction taking place on zirconia surfaces modeled by monoclinic and tetragonal clusters. In order to understand the charge transfer between the active species, in this work we analyze the influence of the geometry of monoclinic and tetragonal zirconia using reactivity descriptors such as electronic chemical potential (μ), charge transfer ($|\Delta N|$) and molecular hardness (η). We have found that the most preferred surface is tetragonal zirconia ($tZrO_2$) indicating also that low charge transfer systems will generate less stable intermediates, that will allow to facilitate desorption process.

Keywords DFT · Dual index · Zirconia

Introduction

The water gas shift reaction $CO + H_2O \rightarrow H_2 + CO_2$ is an excellent via for elimination of carbon monoxide in methanol synthesis and decomposition. This reaction occurs at high temperatures on zirconia (ZrO_2) catalytic surfaces [1]. The catalytic activity has been reported to be dependent on the polymorphic structure of ZrO_2 [2], and activity has also been demostrated to be strongly dependent on the metal adsorbed [3, 4], in this context it has been reported that when copper is used supported on tetragonal zirconia $tZrO_2$ reactivity or CO conversion is much higher than when supported on monoclinic $mZrO_2$ [5, 6], indicating that in water gas shift reaction, the influence of the crystalline structure plays an important role in the activity of the catalyst since intermediates species like formates appear to be interacting with the zirconia support while copper is more active in the dehydrogenation step of the reaction [7].

Experimentally, it has been observed that the differences between the monoclinic and tetragonal support zirconia can be attributed to the high reactivity of the hydroxyl groups [8, 9] attached to the zirconia surface and to anionic defects [8] on them; the latter are mostly found on $mZrO_2$ allowing the generation of bidentate formate groups facilitating the CO adsorption and the formation of stable intermediates [8].

About the bonding of intermediate species experimental results indicate that, the te–tra–gonal support $tZrO_2$ present bonds less stable linked to the surface, whereas monoclinic support $mZrO_2$ may lead to quite stable intermediates attached to the surface [7, 10], this would explain why it is better in the production of CO_2 and H_2 the support on $tZrO_2$ than $mZrO_2$.

Theoretically, there are few works that study the ZrO_2 behavior along the study of a reaction mechanism using plane waves [11] and some using cluster approaches on the analysis of the importance of morphology on catalytic zirconia [12–16]. In this work we provide a new viewpoint to understand the charge transfer process taking place between the adsorbates of the water gas shift reaction in gaseous state and the $mZrO_2$ and $tZrO_2$ supports; the idea is to establish the role of the adsorption and desorption processes. From density functional theory (DFT) [17] it is possible to find rigorous mathematical definition of reactivity descriptors such as chemical potential (μ), electronegativity (χ) and hardness (η) [17–22]. These descriptors are well established global quantities in chemical reactivity studies and are going to be used in this work to characterize the interaction between adsorbates and the clusters of zirconia to characterize the electronics effects observed in these systems [23].

All the systems were calculated using cluster models, to keep consistency with experimental studies on catalytic activity, we

M. L. Cerón · P. Araya · F. Gracia
CIMAT, Laboratorio de Catálisis, Facultad de Ciencias Físicas y Matemáticas, Universidad de Chile, 8320000 Santiago, Chile

M. L. Cerón · B. Herrera (✉) · A. Toro-Labbé (✉)
Laboratorio de Química Teórica Computacional (QTC), Facultad de Química, Pontificia Universidad Católica de Chile, 7820426 Santiago, Chile
e-mail: bherrera@uc.cl
e-mail: atola@uc.cl

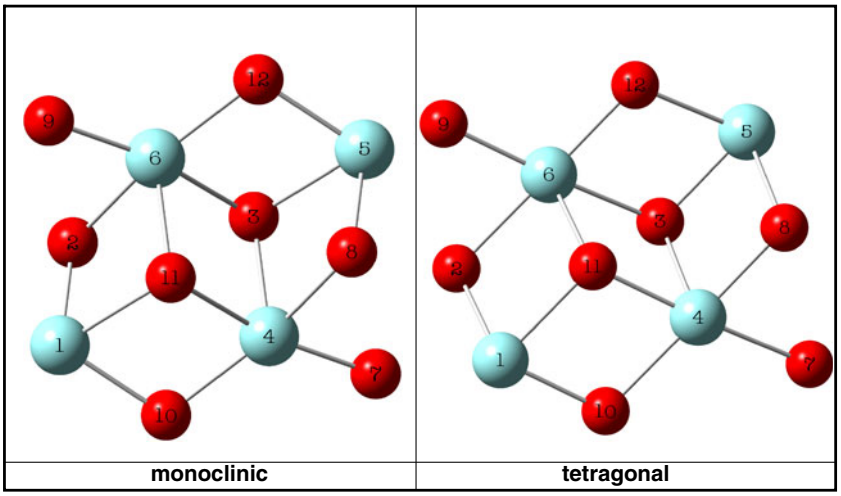

Fig. 1 Models for different phase of ZrO_2, these models represent a cluster of Zr_4O_8

have added hydroxyl groups (OH) to zirconia models imitating the morphology and the species that are present at experimental level, for the modeling of the morphologies we have used geometries coming from x-ray experimental data [11, 24].

In the next section we present a summary of the theoretical elements we use here and the details of the calculations followed by the results and discussion, and finally a few concluding remarks are drawn.

Theoretical background

In DFT the chemical potential, a global electronic property, describes the reactivity of molecular systems, it is defined as: [17–21]

$$\mu = \left(\frac{\partial E}{\partial N}\right)_{v(\mathrm{r})} = -\chi, \tag{1}$$

where (χ) is the electronegativity [19, 20]. This descriptor represents the escaping tendency of the electronic cloud from equilibrium [18]. The second derivative of the energy is known as the chemical hardness, which can be interpreted as the resistance of a chemical system to deform its electronic distribution, it is given by: [17–21]

$$\eta = \frac{1}{2}\left(\frac{\partial^2 E}{\partial N^2}\right)_{v(\mathrm{r})}. \tag{2}$$

Both properties can be obtained numerically through the use of the finite difference approximation [17, 25] and Koopmans [26] theorem, these lead to the following working expressions for μ and η:

$$\mu \approx -\frac{I+A}{2} = \frac{\in_L + \in_H}{2} \tag{3}$$

$$\eta \approx \frac{I-A}{2} = \frac{\in_L - \in_H}{2}, \tag{4}$$

where I is the first ionization potential, A is the electron affinity, $\in_H$ is the energy of the highest-occupied molecular orbital (HOMO) and $\in_L$ is the energy of the lowest-unoccupied molecular orbital (LUMO).

A quantitative estimation of the charge transfer between reacting species A and B is given by: [21, 22].

$$\Delta N = \frac{1}{2}\frac{(\mu_A - \mu_B)}{(\eta_A + \eta_B)}, \tag{5}$$

where $\{\mu_A, \eta_A\}$ and $\{\mu_B, \eta_B\}$ are the chemical potential and hardness of species A and B, respectively [22]. This last Eq. is valid under the condition that the external potential does not vary or it is neglectable in constrast to the variations of the total number of electrons at the reaction coordinate.

The adsorption energies were calculated using a simple model as is presented in the following Eq.:

$$E_{ads} = E_{SM} - (E_{ZrO2} + E_{AD}). \tag{6}$$

In this equation, E_{SM} corresponds to any intermediate or product of the adsorption process considered in this work,

Table 1 Experimental x-ray data on monoclinic and tetragonal zirconia taken from references [11, 24]

Space group	Monoclinic P 2_1/c	Tetragonal P4_2/nmc
Cell parameter (Å°)	a 5.5110 (4)	3.6019
	b 5.2031 (4)	3.6019
	c 5.3151 (4)	5.174
Cell angle	α=γ=90° β=99.197°	α=γ=β=90°

Table 2 Obtained reactivity parameters for monoclinic and tetragonal zirconia clusters at MP2/LanL2Dz/6-31G

Electronic		
Properties (eV)	Monoclinic	Tetragonal
μ	−5.18	−4.28
η	3.10	1.97
IP	8.28	6.25
EA	2.09	2.30

E_{ZrO2} is the energy of bare zirconia presented in its two morphologies and E_{AD} is the energy of the adsorbates that contain the supermolecule (OH, CO or H_2O).

Computational details

All calculations were performed using the *Gaussian−03* (*revision D.02*) [27] package. The clusters representing monoclinic and tetragonal ZrO_2 were built up using x-ray diffraction (DRX) experimental data [11, 24], and shown in Fig. 1. The *OH* species attached to the clusters were optimized at the MP2 level with standard 6–31G basis set and Lanl2DZ pseudopotential [28–30] at zirconium atoms, leaving fixed the coordinates of the isolated clusters. For estimating the $|\Delta N|$ on the different reactions and support geometries, we used the individual optimized adsorbate geometries and zirconia support morphologies (monoclinic and tetragonal) and applied Eq. 5. Once we decided which were the most reactive systems, we did the optimization of each reaction, partially optimizing each stationary point of both reactions at MP2 level, leaving the clusters and OH geometries previously obtained fixed, using the same basis sets (6–31G and LanL2DZ). The molecular vibrations and the population analysis using NBO, were determined using single point calculations at HF level.

Results and discussion

Hydroxyl group in monoclinic and tetragonal clusters

Figure 1 displays models for the different types of ZrO_2 used to describe monoclinic and tetragonal models for the studied reactions, before the OH adsorption. All the cell parameters are depicted in Table 1. We have obtained that $E_m<E_t$ gives more stability to the first system, in agreement with other theoretical and experimental results [6, 31].

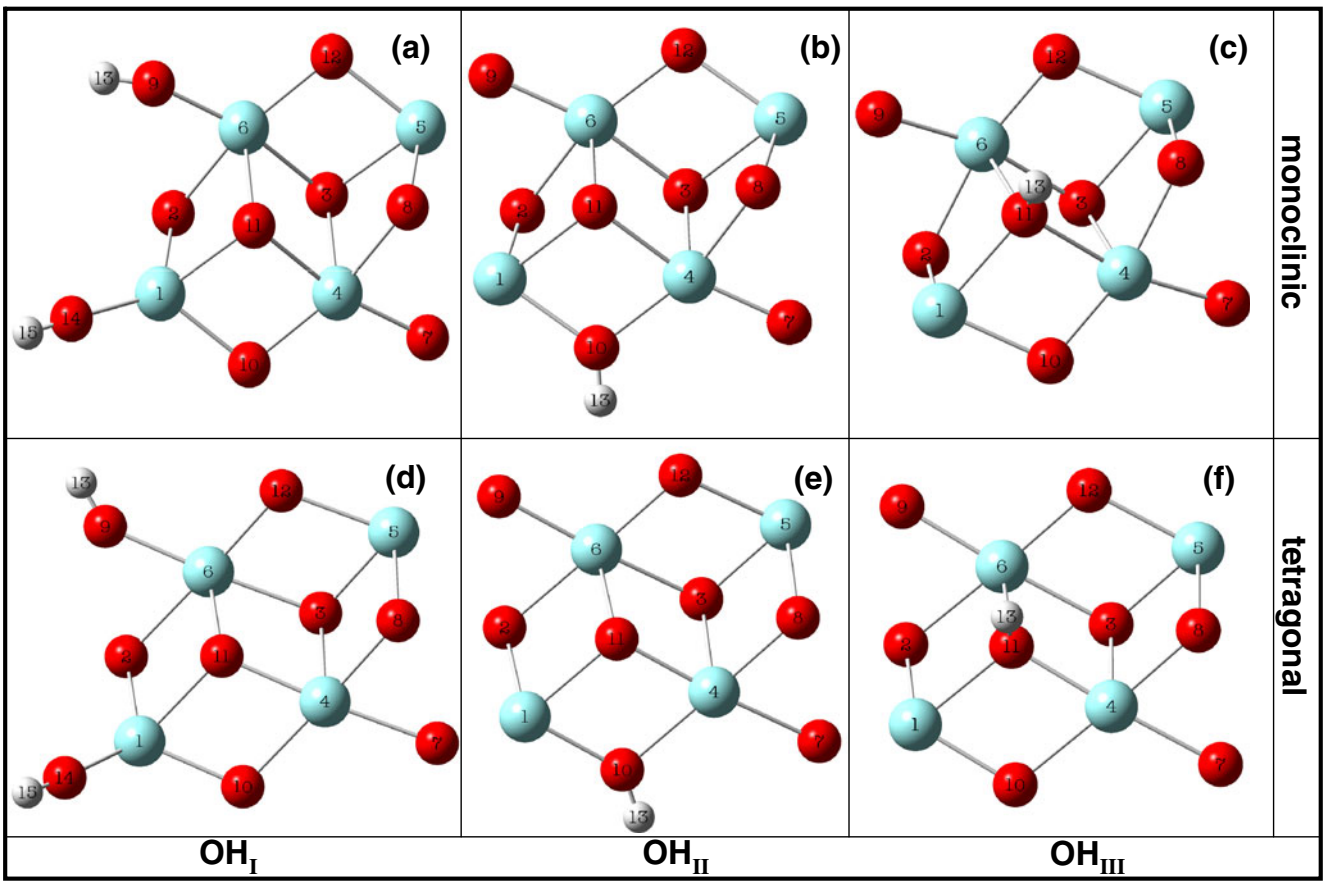

Fig. 2 Scheme of different OH arrangements in monoclinic and tetragonal cluster

Additionally, we have obtained the same electronic properties for this systems, shown in Table 2 the reported values indicate that the reaction changes along morphology, explaining to some extent the diferences in reactivity on methanol reforming. Figure 2 shows models of the hydroxyl groups adsorbed on $mZrO_2$ and $tZrO_2$. The OH arrangements named $(OH)_I$, $(OH)_{II}$ and $(OH)_{III}$, represent apical, bridged and three fold coordination to Zr atoms, respectively. In Table 3 we report the adsorption energies calculated, vibrational frequencies and force constants were calculated at the Hartree-Fock level.

In Table 3, the results indicate that it can be observed that force constants decrease with the coordination of the hydroxyl group, where lower OH coordination indicates that it is firmly attached to ZrO_2 and less deformable than highest OH coordination, in agreement with the adsorption energies calculated for this systems. It is well known that the OH force constants are related to acidity behavior at this groups, indicating that strong Zr-O bonds make the OH proton less acidic in constrast to weak Zr-O bonds. This observation is in agreement with the experimental data of acidity of OH indicating that the tetragonal system is the most acidic, and thus consistent with higher force constants observed in the $(OH)@mZrO_2$ systems [7].

As a second observation, when analyzing the three different types of OH coordinations, the force constants at the Zr-O bond at the hidroxyl moiety decrease with the coordination of the ZrO_2 indicating that the Zr-OH single bond is quite strong and slightly deformable; in contrast, double and triple coordination increases the acidity making the hydroxyl much more reactive. The values for the frequencies obtained are consistent with the experimental data [32]: $(OH)_I@mZrO_2$ vibrate between $3733\,cm^{-1}$ and $3822\,cm^{-1}$, $(OH)_{II}@mZrO_2$ lies in the range $3568\,cm^{-1}$ and $3755\ cm^{-1}$ and $(OH)_{III}@mZrO_2$ between 3498 cm^{-1} and 3647 cm^{-1}. In the tetragonal system experimental data reports indicate a controversy about the assignment of the coordination species, many authors have assigned a range between [9] 3390 cm^{-1} and 3733 cm^{-1}. On the other hand, the actives species in the infrared spectrum for ZrO_2 systems are $(OH)_{II}$ and $(OH)_{III}$ in both phases commonly reported [33, 34]. However, it is possible to observe all the species in both spectrums although $(OH)_I@mZrO_2$ has not been observed at experimental level, one reason of this absence might be masked by other molecular vibrations, being not possible to be reported.

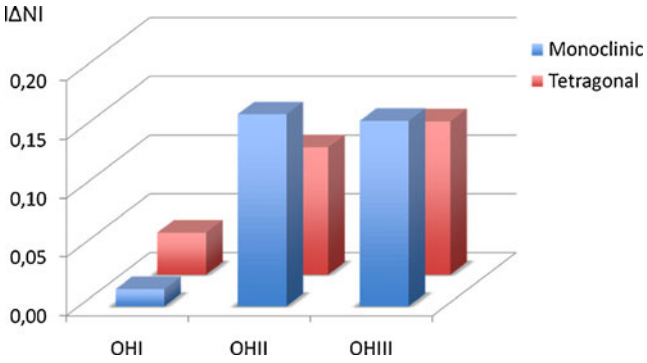

Fig. 3 Adsorption in monoclinic and tetragonal cluster $|\Delta N|$ versus OH arrangements

Charge transfer criteria to describe the influcence of OH geometry in monoclinic and tetragonal clusters

The water gas shift reaction on ZrO_2 can be characterized through the analysis of its two determinant steps:

i) *Adsorption of the reactants*: $(OH)_nZrO_2 + yCO + zH_2O \rightarrow (CO)_y(H_2O)_z \cdots (OH)_nZrO_2$.

ii) *Desorption of the products*: $(H_2)_y(CO_2)_z \cdots (OH)_nZrO_2 \rightarrow yH_2 + zCO_2 + (OH)_nZrO_2$.

The following results are going to be discussed based on those two fundamental steps. For this analysis, we have used the $|\Delta N|$ descriptor calculated from μ and η values that in turn have been determined calculated from the HOMO and LUMO molecular orbital energies using Sanderson's approach for $|\Delta N|$, where the adsorbates and the cluster were considered as a sum of individual fragments in order to discriminate the most reactive system prior to model the complete reaction. It is confirmed that the adsorption energies give quite consistent results with charge transfer, μ and η values, as was obtained in previous sections, so the results will be analyzed using this criteria. In this context, high values of $|\Delta N|$ indicate high tendency to charge transfer and bond forming, lower values indicate the inability to form bonds.

Table 3 Adsorption energies (keV), frequencies in (cm^{-1}) and force constant in $\left(\frac{mdyne}{A}\right)$ of the monoclinic and tetragonal clusters. The frequencies in parentheses correspond to experimental data

$OH@m-ZrO_2$	E_{ads}	Freq	F. const.	$OH@t-ZrO_2$	E_{ads}	Freq.	F. const.
$(OH)_I$	−0.02	3778 (3743–3822)	11.11	$(OH)_I$	−0.02	3718	10.75
$(OH)_{II}$	2.05	3550 (3568–3755)	9.78	$(OH)_{II}$	2.07	3565	9.86
$(OH)_{III}$	2.04	3475 (3498–3647)	9.36	$(OH)_{III}$	2.07	3347	8.68

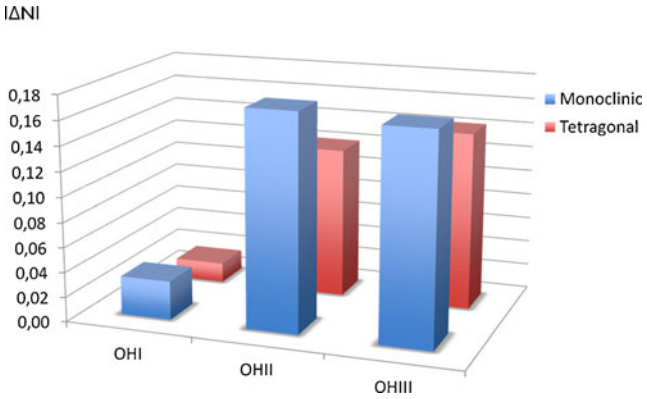

Fig. 4 Desorption in monoclinic and tetragonal cluster $|\Delta N|$ versus OH arrangements

Adsorption of reactants

Figure 3 displays the amount of charge $|\Delta N|$ transferred between the host cluster $(OH)_n - mZrO_2$ and $(OH)_n tZrO_2$ with CO and H_2O adsorbed. This results show that in clusters with $(OH)_{II}$ and $(OH)_{III}$ the charge transfer is larger in the monoclinic system than in the tetragonal system, large blue bars indicate that the interaction adsorbates-support is stronger in the monoclinic clusters. It should be noticed that the highly coordinated group $(OH)_{III}$ produces a strong interaction with the ZrO_2 leading to stable intermediates adsorbed on both clusters although in monoclinic system this can be even higher.

Desorption of products

In Fig. 4 it can be observed form the comparison between $|\Delta N|$ associated to the different OH arrangements in both ZrO_2. In this part of the reaction it is necessary to have a weak interaction with the support in order to favor the dehydrogenation, therefore a lower charge transfer between support and products must be expected. The results show that red $tZrO_2$ bars are smaller than blue $mZrO_2$ bars indicating that the interaction is weaker in tetragonal systems, this phase being the best for the dehydrogenation. In relation with all OH arrangements considered, it is observed that the hydroxyls groups show the same behavior presented in the adsorption analysis, however low coordination would increase the generation of less stable intermediates thus favoring dehydrogenation.

Intermediates and energies in monoclinic and tetragonal clusters

To evaluate the generation of intermediates on ZrO_2 we only considered the clusters $(OH)_{III}@mZrO_2$ and $(OH)_{III}@tZrO_2$

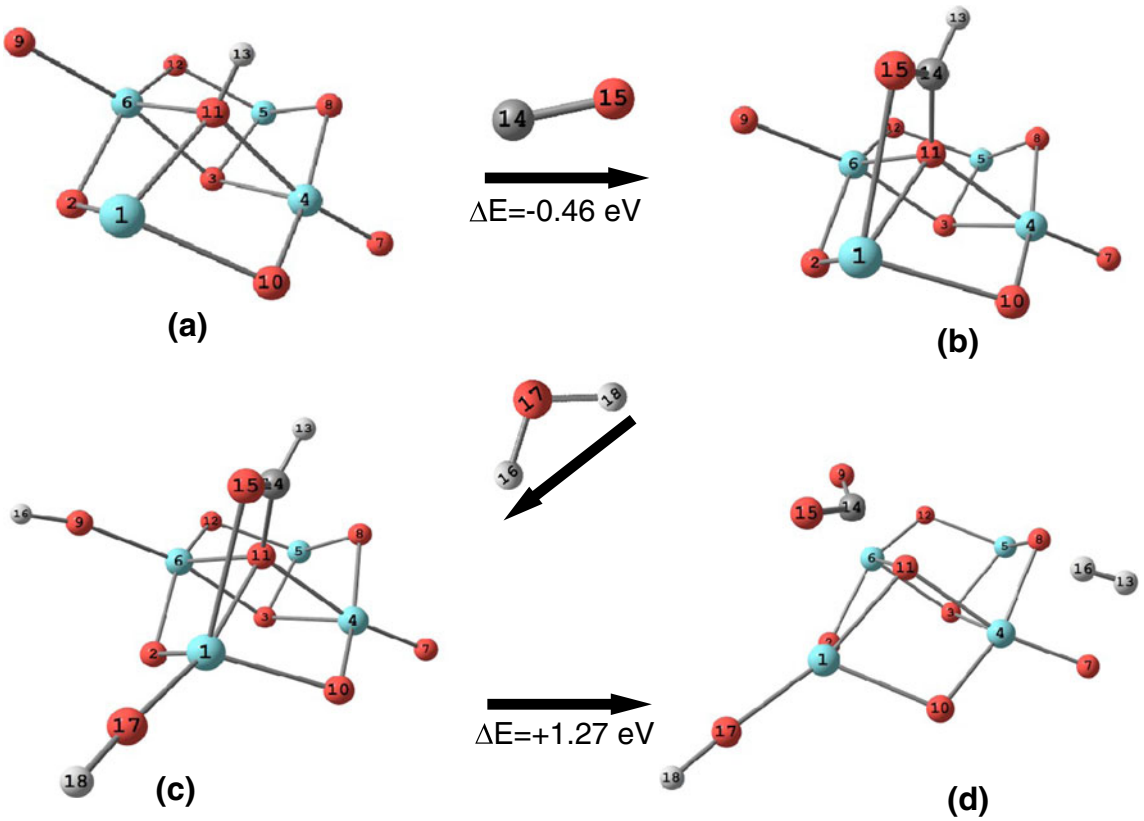

Fig. 5 Evaluating of the reaction WGS on $(OH)_{III}@mZrO_2$

due to they present an active reactant behavior according to our $|\Delta N|$ results and also are consistent to experimental infrared spectroscopy results [32]. The mechanisms for adsorption and desorption together with energies involved are reported in Figs. 5 and 6, all this results are going to be analyzed along with vibrational frequencies.

Adsorption of reactants

The adsorption of carbon monoxide on the composite clusters $(OH)_{III}@mZrO_2$ and $-(OH)_{III}@tZrO_2$ after the adsorption of a water molecule is observed in Figs. 5a and 6a, respectively considering the scheme (*i*) depicted in section "Charge transfer criteria to describe the influence of OH geometry in monoclinic and tetragonal clusters". In this figure is possible to note that the monoclinic system forms bidentate intermediates (Fig. 5b) with an energy gain of 0.59 eV and a E_{ads} of 3.21 eV, this intermediate has been reported as a stable one in the methanol reforming and it is observed [10] at 1575 cm^{-1} which is quite close to our theoretical result of 1596 cm^{-1}. For the tetragonal system a two-steps adsorption process leads to a stable complex with an energy gain of 0.57 eV and a E_{ads} of 3.23 eV. The intermediate is reached after adsorption of *CO* followed by a rearrangement in which bidentate intermediate (Fig. 6c) is generated with an energy loss of 0.84 eV, this intermediate is similar to the one generated in the monoclinic system. This result along with the charge transfer might explain that tetragonal system generates intermediates which are less stable than those on the monoclinic system, in direct relation with the dehydrogenation process because the intermediate-support interactions are weaker and the products are easily detached.

Desorption of products

The desorption of products is related to the scheme of section "Charge transfer criteria to describe the influence of OH geometry in monoclinic and tetragonal clusters" (*ii*) as the release of H_2 and CO_2 from the catalytic surface. According to our results, the monoclinic system does not release the species (Fig. 5d) while in tetragonal system (Fig. 6e) the desorption is favored with an energy gain of 0.13 eV. This might explain the observed trends on charge transfer, where tetragonal system shows more stability at desorption, indicating a weak surface-adsorbate interaction, allowing the release of the species, while monoclinic system

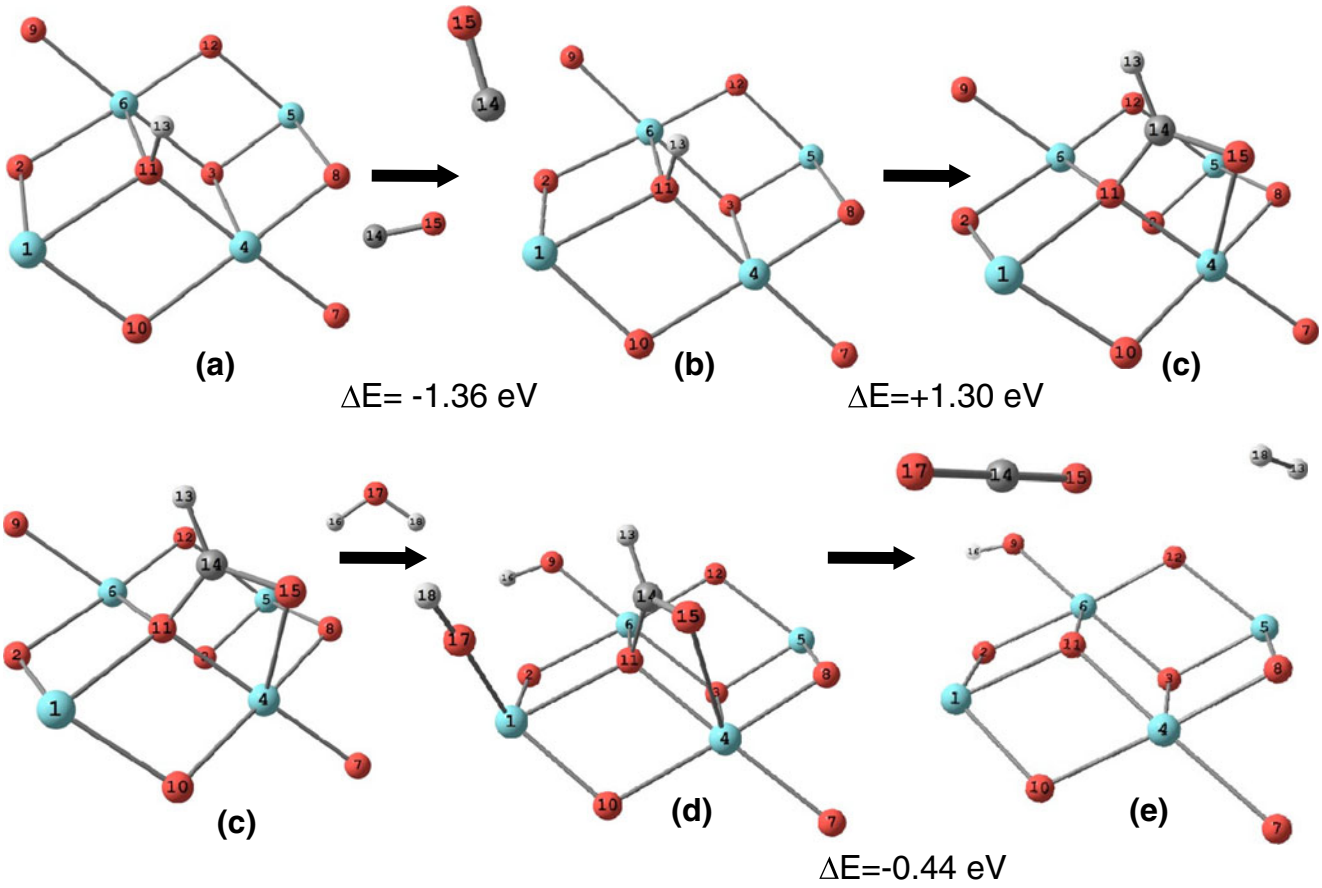

Fig. 6 Evaluating of the reaction WGS on $(OH)_{III}@tZrO_2$

shows higher $|\Delta N|$ values indicating species that prefer to remain adsorbed.

Conclusions

A theoretical study of the influence of the monoclinic and tetragonal zirconia phases on the water gas shift reaction has been presented. In this work, we have used theoretical tools to understand the adsorption and desorption process along zirconia morphology and the OH groups adsorbed in the different geometries, in this context, adsorption energies, μ, η and $|\Delta N|$ demonstrated to be powerful tools indicating the stability of the adsorbed and desorbed species at each system.

Results are in agreement with experimental data for adsorption and desorption processes of the reactant and product species participant in the reaction. It has been found that stable intermediaries are found in monoclinic system, this prevents the release of H_2 and CO_2; in the tetragonal system the adsorption is not facilitated but the desorption is favored with an energy gain of 0.13 eV, this result indicates that low charge transfer will generate less stable intermediates, that will easily allow the desorption process.

Acknowledgments This work was supported by Fondo de Ciencia y Tecnología (FONDECYT) under grants Nº 1090460 and Nº 1120093, Fondo de Areas Prioritarias (FONDAP) Project Nº 11980002 (Centro Interdisciplinario de Materiales (CIMAT)). María Luisa Cerón wants to thank Santander-Universia for a Doctoral fellowship.

References

1. Rhodes MD, Bell AT (2005) J Catal 233:198–209
2. Shukla S, Seal S, Vij R, Rahman Z (2002) Nano Lett 2(9):989
3. Sloczynski J, Grabowski R, Kozlowska A, Olszewski P, Stoch J, Skrzypek J, Lachowska M (2004) App Catal A General 278 (1):11
4. Tsoncheva T, Ivanova L, Paneva D, Mitov I, Minchev C, Froeba M (2009) Microporous Mesoporous Mater 120:389
5. Águila G, Guerrero S, Araya P (2008) Catal Comm 9:2550–2554
6. Aguila G, Guerrero S, Araya P (2008) Catal Comm 9:2550
7. Pokrovski K, Jung KT, Bell AT (2001) Langmuir 17:4297–4303
8. Rhodes MD, Pokrovski KA, Bell AT (2005) J Catal 233:210–220
9. Hertl W (1989) Langmuir 5:96–100
10. Korhonen ST, Calatayud M, Krause OI (2009) J Phys Chem C 112:16096–16102
11. Walter EJ, Lewis SP, and Rappe AM (2001) Surf Sci p. 44
12. Khaliullin RZ, Bell AT (2002) J Phys Chem B 106:7832
13. Foschini C, Treu O, Juiz SA, Souza AG, Oliveira JBL, Longo E, Leite ER, Paskocimas CA, Varela JA (2004) J Mat Sci 39:1935
14. Mantz YA, Gemmen RS (2010) J Phys Chem C 114:8014
15. Milman V, Perlov A, Refson K, Clark SJ, Gavartin J, Winkler B (2009) J Phys Condens Matter 21:485404
16. Herrera B, Gracia F, Araya P, Toro-Labbé A (2009) J Mol Model 15:405
17. Parr RG, Yang W (1989) Density Functional Theory of Atoms and Molecules. Oxford University Press, New York
18. Parr RG, Yang W (1995) Annu Rev Phys Chem 46:701
19. Parr RG, Pearson RG (1983) J Am Chem Soc 105:7512
20. Jorgensen CK, Electronegativy. In: K.D Sen (ed) Structure and Bonding: chemical hardness. Berly, Germany
21. Sanderson R (1955) Sciencie 122:207
22. Gutiérrez-Oliva S, Jaque P, Toro-Labbé A (2000) J Phys Chem A 104:8955
23. Herrera B, Toro-Labbé A, Gracia F, Araya P (2009) J Mol Model 15:405
24. Howard CJ, Hill RJ, Riechert BE (1998) Acta Crystallogr B 44:116
25. Geelings P, De Proft F, Langenaeker W (2003) Chem Rev 103:1793
26. Janak JF (1978) Phys Rev B 18:7165
27. Frisch MJ, Trucks GW, Schlegel HB, Scuseria GE, Robb MA, Cheeseman JR, Montgomery JA Jr, Vreven T, Kudin KN, Burant JC, Millam JM, Iyengar SS, Tomasi J, Barone V, Mennucci B, Cossi M, Scalmani G, Rega N, Petersson GA, Nakatsuji H, Hada M, Ehara M, Toyota K, Fukuda R, Hasegawa J, Ishida M, Nakajima T, Honda Y, Kitao O, Nakai H, Klene M, Li X, Knox JE, Hratchian HP, Cross JB, Bakken V, Adamo C, Jaramillo J, Gomperts R, Stratmann RE, Yazyev O, Austin AJ, Cammi R, Pomelli C, Ochterski JW, Ayala PY, Morokuma K, Voth GA, Salvador P, Dannenberg JJ, Zakrzewski VG, Dapprich S, Daniels AD, Strain MC, Farkas O, Malick DK, Rabuck AD, Raghavachari K, Foresman JB, Ortiz JV, Cui Q, Baboul AG, Clifford S, Cioslowski J, Stefanov BB, Liu G, Liashenko A, Piskorz P, Komaromi I, Martin RL, Fox DJ, Keith T, Al-Laham MA, Peng CY, Nanayakkara A, Challacombe M, Gill PMW, Johnson B, Chen W, Wong MW, Gonzalez C, Pople JA (2004) Gaussian 03, Revision C.02. Gaussian, Inc, Wallingford
28. Hay PJ, Wadt WR (1985) J Chem Phys 82:270
29. Hay PJ, Wadt WR (1985) J Chem Phys 82:284
30. Hay PJ, Wadt WR (1985) J Chem Phys 82:299
31. Terki R, Bertrand J, Aourag H, Coddet C (2006) Mat Sci Semicond Proc 9:1006
32. Korhonen ST, Calatayud M, Krause OI (2008) J Phys Chem C 112:6469
33. Jung KT, Bell AT (2000) J Mol Catal 163:27
34. Bachiller-Baeza B, Rodriguez-Ramos I, Guerrero-Ruiz A (1998) Langmuir 14:3556